Title
Modifier loci condition autoimmunity provoked by Aire deficiency

Journal
Journal of Experimental Medicine, 202(6)

ISSN
0022-1007

Authors
Jiang, Wenyu
Anderson, Mark S
Bronson, Roderick
et al.

Publication Date
2005-09-19

DOI
10.1084/jem.20050693

Peer reviewed

Modifier loci condition autoimmunity provoked by Aire deficiency

Wenyu Jiang,[1] Mark S. Anderson,[1] Roderick Bronson,[2] Diane Mathis,[1] and Christophe Benoist[1]

[1]Section on Immunology and Immunogenetics, Joslin Diabetes Center, Department of Medicine, Brigham and Women's Hospital, Harvard Medical School, Boston, MA 02215
[2]Harvard Medical School, Boston, MA 02115

Loss of function mutations in the *autoimmune regulator* (*Aire*) gene in autoimmune polyendocrinopathy-candidiasis-ectodermal dystrophy patients and mutant mice lead to autoimmune manifestations that segregate as a monogenic trait, but with wide variation in the spectrum of organs targeted. To investigate the cause of this variability, the *Aire* knockout mutation was backcrossed to mice of diverse genetic backgrounds. The background loci strongly influenced the pattern of organs that were targeted (stomach, eye, pancreas, liver, ovary, thyroid, and salivary gland) and the severity of the targeting (particularly strong on the nonobese diabetic background, but very mild on the C57BL/6 background). Autoantibodies mimicked the disease pattern, with oligoclonal reactivity to a few antigens that varied between Aire-deficient strains. Congenic analysis and a whole genome scan showed that autoimmunity to each organ had a distinctive pattern of genetic control and identified several regions that controlled the pattern of targeting, including the major histocompatibility complex and regions of *Chr1* and *Chr3* previously identified in controlling type 1 diabetes.

CORRESPONDENCE
Christophe Benoist
and Diane Mathis:
cbdm@joslin.harvard.edu

Abbreviations used: AIRE, autoimmune regulator; APECED, autoimmune polyendocrinopathy-candidiasis-ectodermal dystrophy; autoAb, autoantibody; BALT, bronchial-associated lymph tissue; LOD, logarithm of the odds; NOD, nonobese diabetic; SNP, single nucleotide polymorphism; T1D, type 1 diabetes.

Most autoimmune diseases arise from a complex interplay between environmental and genetic factors, resulting in a break in immune self-tolerance. Environmental factors have been suspected from epidemiological evidence, in particular because of the striking north/south gradient in the susceptibility to autoimmune diseases (1). Common autoimmune disorders in humans such as type 1 diabetes (T1D), rheumatoid arthritis, and systemic lupus erythematosus reflect influences of a combination of many genetic factors, and this complex genetic picture in human patients has been supported by results on animal models of autoimmune disease. Mechanistic studies in the animal systems have shown that the genetic variants conditioning autoimmune disease act at several levels of the immunoregulatory cascade that normally enforces self-tolerance. For example, in the nonobese diabetic (NOD) mouse model of T1D, different susceptibility regions (termed *Idd* loci) can affect the ability to clonally delete self-reactive T cell precursors in the thymus (2–5); the ability to present self-antigens and select autoreactive T cells (6–8), peripheral tolerance, and the activity of T cells or molecules with regulatory potential (9–12); or the aggressivity of the lesion (13). Interestingly, congenic or knockout studies in the NOD model have revealed that the NOD genetic background seems to predispose to autoimmune disease, but that the autoimmune target can change when some of the susceptibility loci are altered (14–17).

In contrast, monogenic determinism characterizes autoimmune polyendocrinopathy-candidiasis-ectodermal dystrophy (APECED, also known as APS-1; for review see reference 18), which displays autosomal recessive inheritance. The responsible genetic locus was identified by positional cloning as the gene encoding autoimmune regulator (AIRE), a protein with structural and functional features suggestive of a transcription factor. Mutation of the gene specifying the homologous protein in mice, termed Aire, resulted in multiorgan inflammatory infiltrates and autoantibodies (autoAbs) of diverse specificities (19, 20). Exploration of these mutant animals as a model of APECED revealed that Aire exerts its antiautoimmunity function primarily within thymic epithelial cells

W. Jiang and M.S. Anderson contributed equally to this work.
M.S. Anderson's present address is Diabetes Center, University of California, San Francisco, San Francisco, CA 94143.
The online version of this article contains supplemental material.

and that it does this by inducing the transcription of a large set of genes encoding proteins considered to be tissue specific or tissue restricted (20). In addition, *Aire* controls several genes required for efficient presentation of these self-antigens in the thymus, collectively resulting in poor clonal deletion of self-reactive thymocytes (3, 21, 22). Thus, the working model is that Aire promotes immunological tolerance to self by driving the ectopic expression and presentation of many self-proteins within the thymus and, thereby, the negative selection of developing self-reactive thymocytes (23, 24).

Although the disease is monogenic in transmission, APECED patients show a variable range of pathological manifestations, with each patient presenting a different constellation of affected organs and autoAb specificities. Although certain targets of the autoimmune attack are near constant, such as the adrenal and parathyroid glands, other manifestations are less frequently observed (e.g., thyroiditis or T1D, which present in 2–12% of cases) (25, 26). *Aire* knockout mice reproduced this variability, exhibiting a broad range in the rapidity and severity of disease (19–21), thus leading one to ponder the origin of this variability when the very same mutation brings out different phenotypes in individual mice or patients. The variability is unlikely to stem from the mutations themselves because APECED pa-

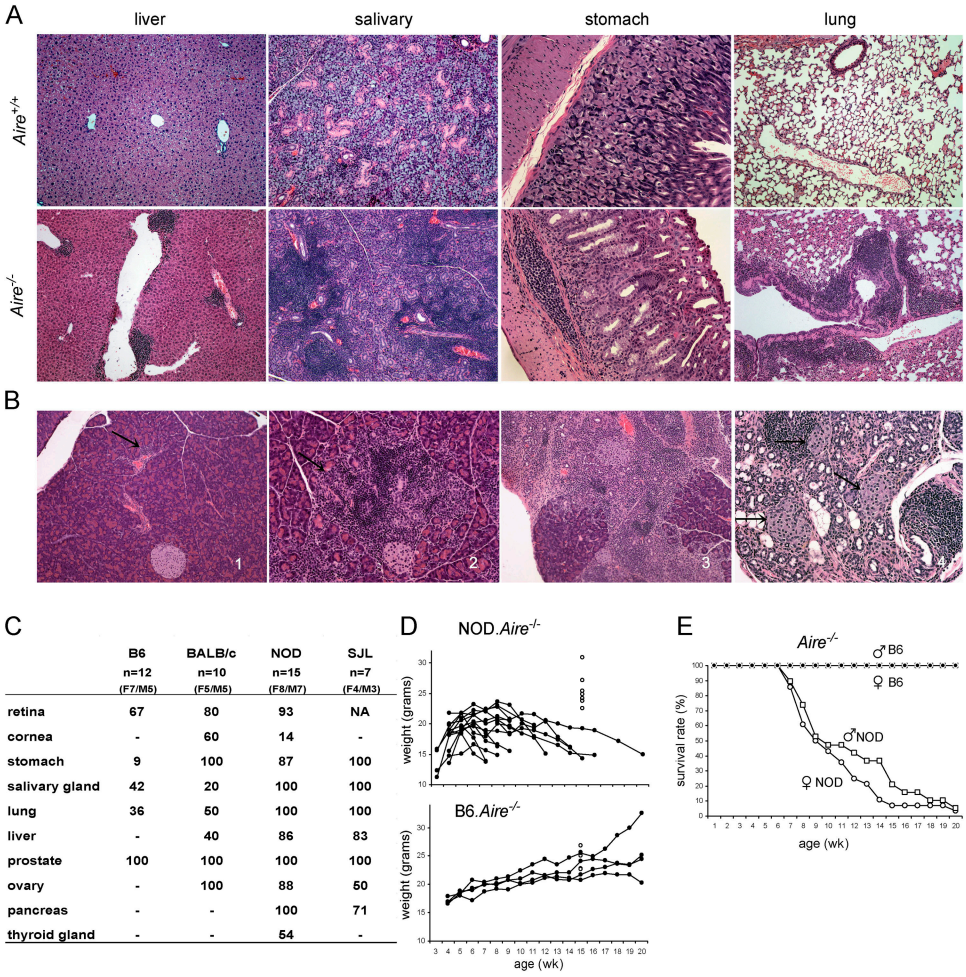

	B6 n=12 (F7/M5)	BALB/c n=10 (F5/M5)	NOD n=15 (F8/M7)	SJL n=7 (F4/M3)
retina	67	80	93	NA
cornea	-	60	14	-
stomach	9	100	87	100
salivary gland	42	20	100	100
lung	36	50	100	100
liver	-	40	86	83
prostate	100	100	100	100
ovary	-	100	88	50
pancreas	-	-	100	71
thyroid gland	-	-	54	-

Figure 1. The genetic background conditions the autoimmunity caused by Aire deficiency. (A) Lymphocytic infiltrates in Aire-deficient mice. Hematoxylin and eosin–stained liver (10× objective), salivary (10×), stomach (20×), and lung (10×) sections from 20-wk-old sex-matched littermates that were *Aire*$^{+/+}$ (top) and *Aire*$^{-/-}$ (bottom) on an NOD (liver, salivary gland, and lung) or BALB/c background (stomach). (B) Pancreatic histology of NOD *Aire*$^{-/-}$ mice at various stages of disease. (1) Perivascular infiltration (arrow), (2) patches of infiltrates (arrow) in exocrine pancreas, (3) massive infiltration in exocrine pancreas, and (4) complete destruction of exocrine pancreas, whereas the islets are spared (black arrows). (C) Percent incidence of disease in different organs in *Aire*$^{-/-}$ mice on B6, BALB/c, NOD, and SJL backgrounds at 20 wk of age. Some of the NOD and SJL background mice were analyzed a few weeks earlier. *n* = total number of knockout mice analyzed. −, no affected mice. Retina refers to retinal degeneration. Except for NOD background mice, in which sialitis was detected in 2/5 *Aire*$^{+/+}$ controls, Aire-proficient littermates showed rare and mild pathology (2/11 lung infiltrates on the B6, 1/5 salivary gland in SJL, and 1/5 ovary in BALB/c backgrounds, respectively). (D) Growth curves of NOD.*Aire*$^{-/-}$ and B6.*Aire*$^{-/-}$ females. Open circles at 15 wk are the weights of groups of *Aire*$^{-/-}$ littermates. (E) Survival of NOD.*Aire*$^{+/+}$ females (open circles) and males (open squares; *n* = 28 and 19, respectively) and B6. *Aire*$^{-/-}$ mice (closed circles and squares; *n* = 7 and 7, respectively).

tients with the same mutation still show phenotypic variability, and the cohorts of Aire-deficient mice all carry the same mutation. One might invoke genetic variation, such as modifier loci affecting the course and targets of the disease; limited data are available, although an association of the HLA complex with actual manifestations has been shown among Finnish APECED patients (27). Alternatively, environmental triggers may precipitate the autoimmune attack against particular organs. Finally, the onset of lesions in APECED patients may be stochastic/chaotic, organ-specific pathology resulting from a threshold of reactivity in the antigen receptor repertoires of T and B lymphocytes.

To address this issue, we explored the influence of genetic background variation on the autoimmune phenotype of Aire-deficient mice. From the original knockout strain, whose analysis had been performed on a mixed genetic background, we crossed the *Aire*-null mutation onto four well-defined inbred backgrounds. The analysis revealed a very strong interaction between the *Aire* mutation and background loci, controlling both the range of target organs and the severity of the resulting autoimmune disease.

RESULTS

Genetic background alters the phenotype of autoimmunity in the absence of Aire

Aire-deficient mice spontaneously develop inflammatory infiltrates in multiple organs that increase with age and are accompanied by autoAbs against distinct structures in the same organs (19, 20). The mice used for the original studies (19–21) were of a mixed (129/Sv × C57BL/6) F2 genetic background, and targeted organs included the salivary gland, ovary, prostate, eye, liver, and stomach, with variability in the penetrance of each organ's attack in different individuals. To systematically test the influence of genetic background on the autoimmune phenotype, we performed parallel backcrosses of the *Aire* knockout mutation onto the C57BL/6J (B6), NOD/LtJ (NOD), BALB/cJ (BALB/c), and SJL/J backgrounds. These well-characterized inbred strains are considered relatively resistant (B6 and BALB/c) or prone (NOD and SJL) to autoimmune disease. After 8–10 generations of backcross, leaving <1% residual heterozygosity, the mice were intercrossed to generate homozygous experimental animals and littermate controls. Mice were aged to 20 wk, the presence of inflammatory infiltrates was analyzed histologically (Fig. 1), and the spectrum of autoAbs was revealed by immunofluoresence on frozen tissue sections (Fig. 2).

The various genetic backgrounds had striking effects on the diseases resulting from the Aire deficiency (Fig. 1, A and B). First, the range of affected organs was quite different. For instance, gastritis was constant in Balb.*Aire*$^-$ mice, but rare in B6.*Aire*$^-$ mice; pancreatitis and thyroiditis were exclusive to NOD.*Aire*$^-$ and SJL.*Aire*$^-$ mice. The distribution of autoAb reactivities also showed clear strain distinctions that correlated, albeit not completely, with strain-specific patterns of organ infiltration (Fig. 2). These patterns of serological reactivity were very reproducible; for example, the discrimination between different salivary glands by NOD.*Aire*$^-$ was found with all these sera (more intense staining of the sublin-

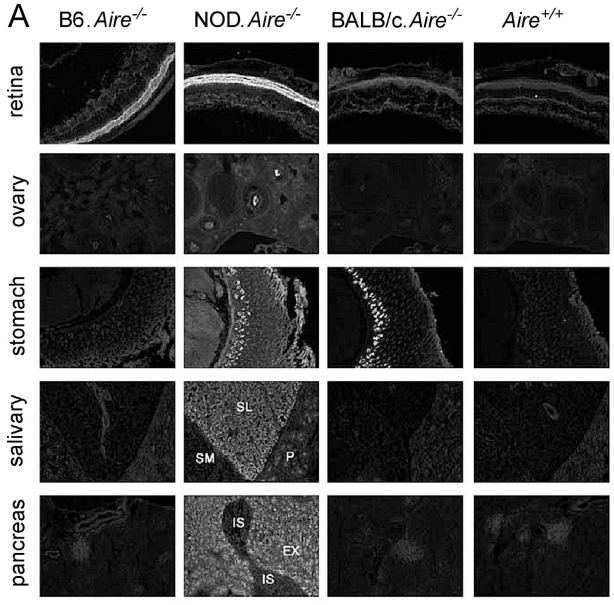

B

strain	sex	pancreas	eye	salivary gland	ovary	stomach
NOD	F	+	+	+	+	+
NOD	F	+	+	+	+	+
NOD	M	+	+	+	-	+
NOD	M	+	+	+	-	+
NOD	M	+	+	+	-	-
NOD	M	+	+	+/-	-	-
B6	F	-	+	-	-	-
B6	F	-	+	-	+	-
B6	F	-	+	+/-	-	-
B6	M	-	+	-	-	-
B6	M	-	+	-	-	-
B6	M	-	-	-	-	-
BALB/c	F	-	+	-	-	+
BALB/c	F	-	+/-	-	-	+
BALB/c	F	-	-	-	-	+
BALB/c	M	-	-	-	-	+
BALB/c	M	-	-	-	-	+
BALB/c	M	-	-	-	-	+

Figure 2. Autoantibodies from Aire-deficient mice of different genetic backgrounds match the disease specificity. (A) Representative staining of frozen sections from retina, ovary, stomach, salivary, and pancreas (10×) of a RAG-deficient mouse with sera from 10-wk-old *Aire*$^{-/-}$ mice from different backgrounds, and an age- and sex- matched *Aire*$^{+/+}$ mouse (B6 background, except for stomach section [BALB/c background]). P, parotid; Sl, sublingual gland; Sm, submandibular gland; Ex, exocrine pancreas; Is, pancreatic islets. (B) Summary of the presence of organ-specific autoAbs to the indicated organs in individual 10-wk-old *Aire*$^{-/-}$ mice from different backgrounds. ±, trace staining.

gual than the parotid or submandibular glands). This analysis also revealed a new target organ, the exocrine pancreas, that had not been observed in the original analysis of knockout mice on the (B6 × 129) F2 background. Aire-deficient mice on both NOD and SJL backgrounds were susceptible to these pancreatic lesions; those on the BALB/c and B6 backgrounds were resistant. Although an involvement of the pancreas was not surprising given the well-known susceptibility of NOD mice to T1D, the focus on exocrine cells was unexpected. As was previously observed (19, 20) and illustrated again by the focal infiltrates in the liver or salivary gland (Fig. 1 A), the lesions were highly localized within the pancreas. According to the analysis of numerous sections, they appeared to progress from an initial extravasation into the perivascular connective tissue (Fig. 1 B, 1 and 2) to a front of cell destruction that moved through the exocrine lobe (Fig. 1 B, 3), ultimately leaving a wasteland of amorphous tissue with duct-like structures (Fig. 1 B, 4). Strikingly, the damage largely spared the islets, and all of the NOD.*Aire*$^{-}$ mice remained normoglycemic (not depicted). This exocrine specificity was also manifest in the autoAbs, which bound abundantly to the exocrine pancreas but not to the islets (Fig. 2, bottom).

Second, the NOD and SJL genetic backgrounds not only brought out new targets, as in the pancreas, but also resulted in more frequent and severe infiltrates in general (Fig. 1 A) and a higher reactivity of serum autoAbs (Fig. 2). Along with an increased frequency of disease in multiple organs, NOD.*Aire*$^{-}$ mice were also prone to weight loss between 5 and 15 wk of age (Fig. 1 D). This runting seemed to correlate best with the intensity of the pancreas or lung lesions and led to early lethality on homozygotes (79% of NOD.*Aire*$^{-}$ mice died spontaneously or had to be killed between 6 and 14 wk of age). Pathological analysis strongly suggests that the lung lesions, with generalized pneumonitis, must be those that provoke the weight loss and lethality in NOD.*Aire*$^{-}$ mice. Anecdotal evidence indicates that Balb.*Aire*$^{-}$ mice are largely free of this phenotype, whereas SJL.*Aire*$^{-}$ appear susceptible.

To investigate the range and specificity of the autoAbs elicited by the Aire deficiency in the various strains, we probed immunoblots of extracts from several tissues with sera from individual Aire-deficient mice on the NOD, B6, and BALB/c backgrounds. As shown in Fig. 3, the autoAb specificities detected by these blots mirrored the histopathology. Sera from NOD.*Aire*$^{-}$ mice showed the broadest reactivity, with staining of every target tissue, and were the only sera that bound to pancreas proteins. Sera from Balb.*Aire*$^{-}$ mice exhibited near-constant reactivity against stomach antigens, with patterns distinctly different from those of sera from NOD.*Aire*$^{-}$ mice. At the other end of the spectrum, sera from B6.*Aire*$^{-}$ mice showed only sporadic and weak reactivity against salivary and gastric antigens. In all cases, these specificities were absent in control Aire-sufficient littermates. The results presented in Fig. 3 also highlighted the oligoclonality of the autoimmune response. Within each strain, sera from individual Aire-deficient mice yielded discrete patterns, with only a limited number of visible bands. The patterns were quite reproducible from one mouse to the next, with frequently recurring bands. The banding patterns varied with the backgrounds and, as better depicted in Fig. 3 B, the autoAb targets were largely tissue specific. Thus, the genetic background

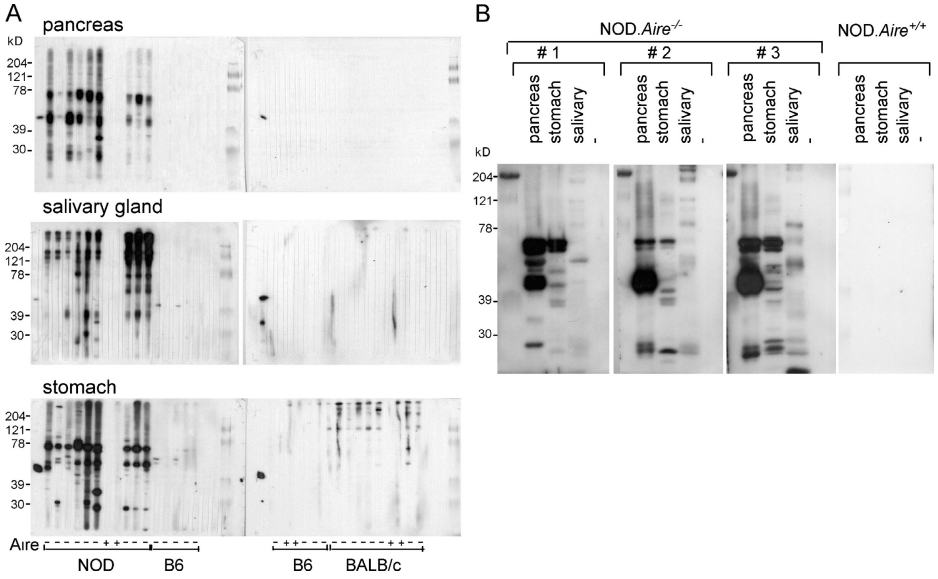

Figure 3. Stronger and different autoAbs in NOD.*Aire*$^{-/-}$ than in other strains. (A) Each lane of the multiscreen immunoblot shows autoAbs in the serum from a 10- or 20-wk-old individual *Aire* $^{-/-}$ mouse (−) or WT littermate (+) on the NOD, B6, or BALB/c background immunoblotted with pancreatic, salivary, or gastric antigens. Anti-β-actin antibody as a positive control is in the first lane of each membrane. (B) Higher resolution immunoblot of autoAb targets in different tissues with sera from three different mice.

controls the general intensity of the autoAb response, as well as the exact self-antigens targeted by serum autoAbs.

Genetic analysis of pancreatitis and gastritis

Next, we asked what modifier loci might underlie these differences and how these regions might relate to regions known to influence spontaneous autoimmune diseases. A series of crosses between the two inbred backgrounds with the most divergent phenotype, B6 and NOD, were performed. This combination was also attractive because of the panels of genotyping reagents, large body of data, and strains of congenic mice accumulated from prior work in many laboratories dissecting diabetes susceptibility loci in this strain combination. We focused on the two phenotypes that were most divergent between these two strains, pancreatitis and gastritis (Fig. 1 B), and analyzed the impact of the Aire deficiency in several congenic lines and in an F2 intercross setting.

Overall, the MHC plays the major role in the genetic determinism of autoimmune disease, and the $H2^{g7}$ haplotype from the NOD mouse is the principal element in diabetes susceptibility, with its impact far outweighing that of any other locus (28). We tested the relative roles of the MHC and the rest of the genome by introducing the *Aire* knockout mutation from NOD.*Aire*$^{-}$ and B6.*Aire*$^{-}$ mice onto a reciprocal congenic pair of strains, NOD.$H2^{b}$ and B6.$H2^{g7}$. For clarity, we have left out the results from Aire-proficient littermate controls, but all manifestations discussed below were strictly dependent on the *Aire*-null mutation (unpublished data). For pancreatitis, a strong influence of the MHC was detected with the NOD-based congenics: the presence of at least one copy of the $H2^{g7}$ haplotype, and preferably two, was required (Fig. 4 A). On the other hand, $H2^{g7}$ was not sufficient because the same MHC haplotypes only led to infrequent disease when combined with B6 alleles at all other loci, i.e., in the B6.$H2^{g7}$ congenic (Fig. 4 B). The same conclusions were reached for autoAb production: the $H2^{g7}$ haplotype at the MHC was necessary on the NOD.*Aire*$^{-}$ background, but was not sufficient on the B6.*Aire*$^{-}$ background (Fig. 4, A and B, bottom).

Outside the MHC, the strongest protection against diabetes in congenic mice is conferred by the *Idd3* and *Idd5* regions on chromosomes 3 and 1, respectively. To test whether these regions could also protect against pancreatitis and gastritis on the NOD background, we backcrossed NOD.*Aire*$^{-}$ mice to the NOD.*Idd3/Idd5* double-congenic line (29, 30). No clear effect of *Idd5* alone was observed (Fig. 4 C). A limited degree of protection was observed with the b/b allele at *Idd3* (Fig. 4 D), but this was pronounced when complemented by the b/b allele at *Idd5* (Fig. 4 E), pointing to synergestic interactions between the loci. Overall, the NOD MHC region is necessary but not sufficient, and other diabetes susceptibility regions also influence the development of pancreatitis in the absence of Aire.

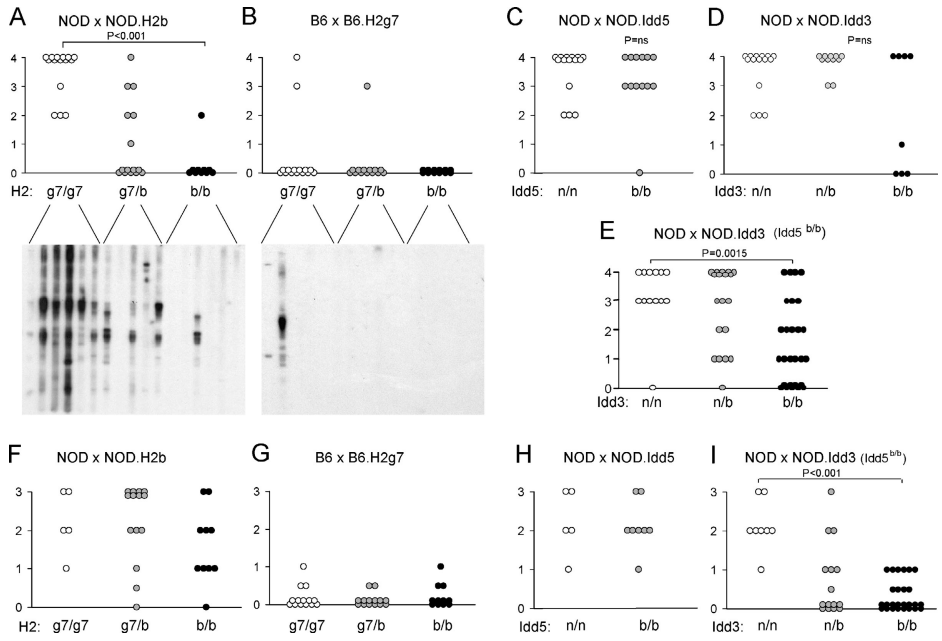

Figure 4. Different NOD congenic intervals influence *Aire*-associated pancreatitis and gastritis. NOD.*Aire*$^{-/-}$ and B6.*Aire*$^{-/-}$ mice were intercrossed with a set of congenic mice with different MHC or Idd intervals. (A, B, F, and G) MHC (reciprocal on B6 and NOD backgrounds). (C and H) *Idd5*^{b} on the NOD background. (D) *Idd3*^{b} on the NOD background. (E and I) *Idd3*^{b} on the NOD.*Idd5*^{b} background. Note that all NOD.*Idd3* mice also carried the B6 allele at *Idd5*. The resulting Aire-deficient homozygous animals, which shared a genetic background except for the indicated genotype at the congenic interval, were scored histologically for pancreatitis (A–E) and gastritis (F–I) at 20 wk of age. Each circle represents an individual *Aire*$^{-/-}$ mouse. Statistical p-values were obtained with a Wilcoxon rank sum test. (A and B, bottom) Immunoblots from sera of animals of the indicated genotypes, probing pancreas extracts.

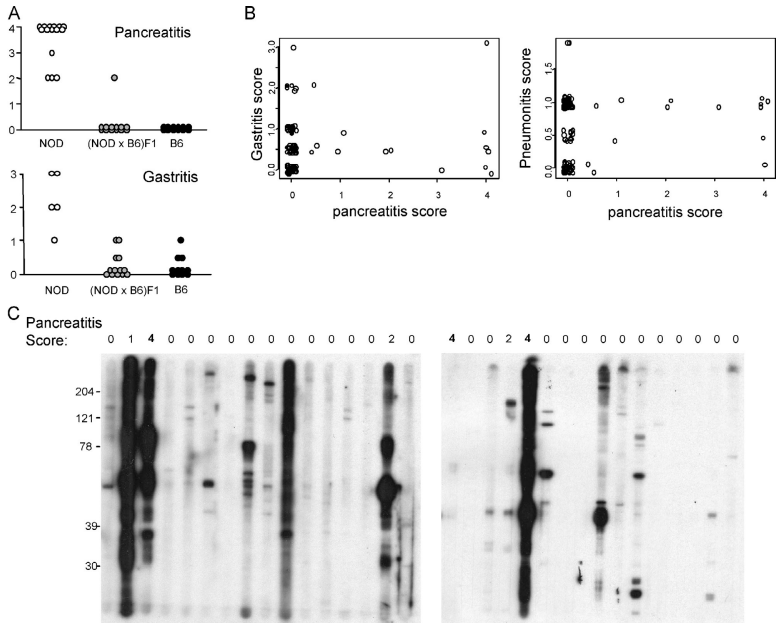

Figure 5. Pancreatitis and gastritis in intercrossed NOD.*Aire*$^{-/-}$ and B6.*Aire*$^{-/-}$ mice. (A) Pancreatitis and gastritis in *Aire*$^{-/-}$ (B6 × NOD) F1 mice. (B) *Aire*$^{-/-}$ (B6 × NOD) F2 mice were generated by intercrossing F1 parents, and the resulting mice were scored for disease. The biparametric plots show scores of individual mice for pancreatitis versus gastritis (left) and pancreatitis versus pneumonitis (right). (C) Antipancreas autoAbs were assayed by immunoblot in sera from (B6 × NOD) F2 *Aire*$^{-/-}$ mice. Each lane corresponds to an individual F2 mouse whose histological pancreatitis score is shown at the top.

Analysis of gastritis in these congenics revealed an effect different from that observed for pancreatitis. The most obvious difference was the absence of MHC association on either the NOD.*Aire*$^{-}$ or B6.*Aire*$^{-}$ backgrounds; animals were equally prone to gastritis whatever their MHC haplotype (Fig. 4, E and F). On the other hand, a protective effect of the B6 alleles at the *Idd3* interval was observed (Fig. 4, G and H), as for pancreatitis.

In a parallel effort to broadly gauge the number and importance of modifier loci that control organ targeting in Aire-deficient mice, we also performed an intercross between NOD.*Aire*$^{-}$ and B6.*Aire*$^{-}$ mice. As shown in Fig. 5 A, both pancreatitis and gastritis were essentially absent in the F1 animals, indicating that susceptibility to these autoimmune manifestations is recessive, a common situation with the genetics of autoimmunity. These (B6 × NOD) F1.*Aire*$^{-}$ mice were then intercrossed, and the resulting (B6 × NOD) F2.*Aire*$^{-}$ animals, whose chromosomes contained random shuffles of the B6 and NOD genomes, were then assayed at 15 wk of age for infiltrates in various organs. As expected, only a minor fraction of the animals presented with pancreatitis or gastritis (Fig. 5 B and Table S1, available at http://www.jem.org/cgi/content/full/jem.20050693/DC1). There was no difference in incidence between genders. In addition, the two diseases were not correlated, as most of the affected mice presented with one or the other lesion and only one mouse with both. Lung and liver infiltrates correlated somewhat, however. Sera from these F2 mice were also tested by immunoblotting against extracts from pancreas (Fig. 5 C). There was a close correlation between the presence of antipancreas autoAbs and of pancreatic infiltrates, as sera from most mice with aggressive pancreatitis gave strong reactivity on the blots (although there were exceptions). A genome-wide scan was then performed on genomic DNA from 98 *Aire*$^{-/-}$ F2 mice, genotyped by fluorogenic PCR for a set of 117 single nucleotide polymorphism (SNP) markers distinguishing the NOD and B6 genomes. The markers covered all 19 autosomes, with an average spacing of ∼16 Mb. Tabulations of the complete marker set and the genotyping results are shown in Table S2. Results from trait/marker association (S-plus, R/qtl) (31) are displayed in Fig. 6 and summarized in Table 1. For pancreatitis, the highest logarithm of the odds (LOD) score was observed for markers on Chr 17, which was consistent with the above-described effect of the MHC in the congenic analysis. Regions on Chr3, 9, and 1 had fairly comparable LOD scores in the "suggestive" range, the former and latter being consistent with the role of *Idd3* and *Idd5* detected in the congenic

Table I. Main associated regions

	Chr	Peak position	Max LOD	Susceptibility allele	Model
		Mb			
Pancreatitis	1	49.89	2.24	NOD	recessive
Pancreatitis	3	114.35	2.59	NOD	additive
Pancreatitis	9	48.92	2.36	NOD	additive
Pancreatitis	13	52.37	1.69	NOD	additive
Pancreatitis	17	32.80	3.3	NOD	additive
Gastritis	3	37.23	5.04	NOD	additive

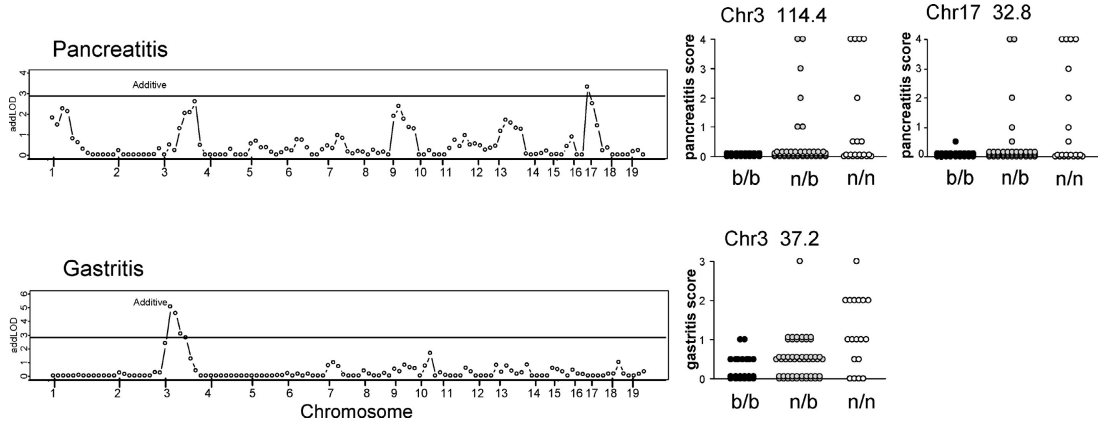

Figure 6. Different genetic regions are associated with pancreatitis and gastritis in *Aire*$^{-/-}$ (B6 × NOD) F2 mice. 98 *Aire*$^{-/-}$ (B6 × NOD) F2 mice were tested histologically and genotyped across the entire genome (117 SNP markers distinguishing NOD and B6 genomes, displayed in chromosomal order). The LOD score is shown for association with pancreatitis (top) and gastritis (bottom). A score of 2.96 corresponds to a genome-wide significance of P = 0.05 (1,000 permutations). (right) Disease scores for animals grouped by genotype at the different markers are shown.

mice. For gastritis, there was a conspicuous absence of any peak on Chr 17, which was again consistent with the congenic results of Fig. 4, but there appeared a very striking linkage on Chr 3. This finding, coupled with the congenic data, suggests that gastritis is not under MHC control but primarily controlled by a region on Chr3. No significant scores ($P < 0.05$ after connection) were obtained for antibody reactivity, perhaps owing to the limited number of animals and to the different subphenotypes present among the antibody reactivity patterns. Finally, salivary gland infiltration showed no evidence of linkage to any region in this cohort of F2 mice (not shown), as might be expected given that there was little difference between the parental strains. Thus, the F2 analysis confirmed that autoimmune attack of different organs in Aire-deficient mice show distinct genetic influences.

DISCUSSION

This study assessed the effect of genetic variation among inbred mouse strains on the autoimmune phenotype provoked by a defective *Aire* gene as a guide to understanding the root of phenotypic variation between APECED patients. Quite clearly, background genes have a strong influence on the overall penetrance of the phenotype, which ranges from fairly mild in B6.*Aire*$^{-}$ mice to lethal in 90% of NOD.*Aire*$^{-}$ mice. Our results are consistent with preliminary observations showing a greater incidence of gastritis in Aire-deficient mice on the BALB/c than on the B6 backgrounds (32). We conclude by analogy that much of the phenotypic variability between APECED patients with the same mutation in the *AIRE* gene must reflect the influence of genetic modifier elements. Because APECED is a fairly rare disease, this contribution would be impossible to track on a genome-wide basis in human patients. The rather mild disease in B6.*Aire*$^{-}$ mice also suggests that some unrecognized individuals might exist, in which some elements of the diagnostic triad (adrenal, parathyroid deficiency, and candidiasis) would be missing because of strongly inhibitory background genes. Indeed, recent clinical reports have described patients with *AIRE*-null mutations and atypical clinical features that do not include the complete triad (33, 34). In addition, the higher prevalence of APECED cases in particular populations (such as Sardinians, Iranian Jews, and Finns) may denote a higher frequency of positively acting alleles in these groups, beyond that of the *AIRE* mutations themselves. It may be no coincidence that these APECED-prone populations are also particularly susceptible to T1D (e.g., Finland and Sardinia); the genetic makeup of these groups, more prone to autoimmunity, may render the severity and detectability of APECED particularly high.

The variation in modifier loci influence the Aire-deficient phenotype in two distinct ways. First, they modify the range of the targeted organs and antigens. For example, the BALB/c background brings out susceptibility to gastritis and oophoritis but not pancreatitis, whereas the NOD and SJL backgrounds bring out susceptibility to gastritis, oophoritis, pneumonitis, and pancreatitis. The fluctuation in the range of antigen targeting is illustrated most graphically by the stomach autoantigens detected on protein blots or tissue sections; the stomach structures and molecular species recognized by sera from Balb.*Aire*$^{-}$ and NOD.*Aire*$^{-}$ mice are clearly different. Second, the genetic variation also determines the overall intensity of the autoimmune reaction: there were more aggressive lesions and higher autoAb production against all organs in NOD.*Aire*$^{-}$ mice. It is certainly no coincidence that the NOD mouse, the most popular mouse model of autoimmune diabetes, would be the most susceptible of the backgrounds tested. NOD mice are known to have defects in the central induction of tolerance by clonal deletion (2–5) and likely in peripheral immunoregulatory pathways as well, although the nature of the latter remains to be established (4, 9, 11, 35). In theory, both levels could contribute; two different deficiencies in thymic clonal

deletion might synergize, or faulty peripheral immunoregulation might further unveil autoreactive T cells that had been improperly tolerized because of a lack of Aire in the thymus. In this respect, it is noteworthy that the NOD background does not broaden the range of protein targets as it intensifies the degree of the autoimmune response. The number of bands on stomach immunoblots is comparable in Balb.*Aire*$^{-}$ and NOD.*Aire*$^{-}$ mice, but their intensities vary. This finding might be more compatible with the second notion, that immunoregulatory defects in NOD mice support a better activation and amplification of autoreactive T cells that are allowed to pass unscathed through the thymus because of the Aire deficiency. Consistent with this idea, we have found in another context that the mechanisms of central tolerance (controlled by Aire) and of peripheral T regulatory cells (controlled by FoxP3) are highly complementary (unpublished data; Chen, Z., personal communication).

The location of the pancreatic autoimmunity in NOD.*Aire*$^{-}$ mice did come as a surprise. We had expected that the Aire deficiency might accelerate the course of spontaneous diabetes in the NOD mouse, particularly because the *Ins-2* gene is one of the principal genes whose ectopic transcription in the thymus is dependent on Aire (20). Yet, not a single NOD.*Aire*$^{-}$ mouse ever became diabetic, and true insulitis was quite rare in NOD.*Aire*$^{-}$ or F2 mice. Part of the explanation may lie in the fact that NOD diabetes is very susceptible to environmental influences (36), and one might propose that the raging exocrine pancreatitis, which occurs quite early, might inhibit the development of insulitis and diabetes. The pancreatic lesions also resemble, in their early phases, those described in aged NOD.B10H2^{b} congenic mice (14). Might there be, in NOD mice, a spontaneous tendency to inflammation in the perivascular tissues of the pancreas, which then focuses on either the endocrine or exocrine components as a function of tolerance defects resulting from MHC or *Aire* variation?

It is also interesting to note that the phenotype of autoimmune exocrine pancreatitis has been suggested in several clinical studies of APECED patients (37, 38). Many APECED patients have chronic malabsorption, and the pancreatitis phenotype of the Aire-deficient mice supports the notion that this process may explain part of the malabsorption syndrome in these subjects.

The pneumonitis and peribronchial infiltrates observed in the NOD.*Aire*$^{-}$ mice were also absent in the original descriptions. It is interesting to note that the NOD genetic background is associated with the development of prominent bronchial-associated lymph tissue (BALT) in aged animals (39). The prominence in BALT was not seen in age-matched Aire-proficient controls in our study because they were analyzed at younger ages (20 wk vs. 1 yr). This predisposition to BALT formation, however, may explain why this phenotype is brought out in the NOD.*Aire*$^{-/-}$ mice.

In all mouse strains examined, the autoimmunity was pauciclonal, focused on a rather limited range of targets with quite reproducible patterns from one mouse to the next. Incidentally, the backcrossing onto inbred backgounds reduced the interindividual variability in the profiles of immunoreactivity observed with the original Aire-deficient (B6 × 129) F2 cohort (unpublished data; Garibyan, L., personal communication). One wonders why such a limited array of antigens is targeted, given that the absence of Aire modifies the ectopic thymic expression of several hundred genes (20, 40). Quite likely, the ability of these self-antigens to be taken up by antigen-presenting cells processed to "presentable" peptides for MHC binding restricts the range of potential targets, much as MHC alleles do in classic autoimmune diseases. It is also possible that dominant autoimmune attacks mask others, much as the exocrine pancreatitis in NOD.*Aire*$^{-/-}$ mice seems to impinge on islet pathology. This implies, then, that even when the immune system is confronted with defective central tolerance to a large number of self-antigens, the constraints on MHC specificity, antigen handling, peripheral tolerance and autoimmune activation can sharply limit the potential damage.

The very nature of the genomic regions implicated in controlling the Aire-negative phenotype in the very concordant analyses in congenic and F2 animals was also somewhat surprising. We had expected to uncover a dominant role for the MHC in targeting the affected organs given its strong association with many autoimmune models. The MHC region did have a clear effect on pancreatitis, with the strongest impact in the congenic analysis, but it was not much greater than were the contributions of other regions on *Chr3* and *Chr9* in the F2 linkage analysis (although the relative contributions of the regions may be somewhat approximate in this instance given the number of mice involved). For gastritis, there was no sign of association with the MHC in either the congenic or F2 Aire-deficient mice. Thus, the influence of MHC alleles, when present, was far from being as overwhelming as it usually is in the susceptibility to classic autoimmune diseases like T1D. This contribution is consistent with the reports of minor influence of the HLA region on the range of affections in APECED patients (27, 41). NOD-derived alleles in the *Idd3* interval on Chr3 were implicated in several instances, predominantly for gastritis, but also for pancreatitis. This effect may represent the contribution of the NOD genome to subvert peripheral tolerance, as discussed above, and may involve the same variant genes that underpin susceptibility to T1D in this strain. This diversity of influences is compatible with the fact that essentially no correlation was found between the autoimmune attacks on different organs in the F2 cohort. One might speculate that these organ-specific influences represent polymorphisms in actual self-antigens or the ability of specific organs to shed antigens in a manner that activates an autoimmune response, much as developmentally programmed apoptosis in pancreatic islet cells initiates the activation of islet-specific autoimmunity (42). Perhaps related, several congenic or knockout variants of NOD mice are protected from diabetes but develop alternate autoimmune dis-

eases such as thyroiditis (15), autoimmune neuropathy (16), or autoimmune biliary disease (17).

There is also an interesting parallel with the range of autoimmune diseases provoked by neonatal thymectomy or Aire deficiency. The neonatal thymectomy model is thought to reflect perturbations in the population of $CD25^+$ T regulatory cells. Neonatally thymectomized BALB/c animals are particularly prone to gastritis (43), which is similar to what we observe in BALB/c.*Aire*$^{-/-}$ mice. This suggests that some of the mechanisms that focus autoimmunity to particular organs may be shared in the two models. Previous work comparing neonatal thymectomy in the BALB/c with the B6 (which are resistant to gastritis) backgrounds has mapped the control of gastritis to chromosome 4 (44), which is different from the chromosomal associations found here. This might indicate that NOD and BALB/c susceptibility to gastritis have different determinism and targets, which is consistent with the different reactivity profiles on the immunoblots. More generally, however, that autoimmune attack on different target organs is determined by specific genetic regions may be a theme common to defects in central tolerance, as in Aire-deficiency, and to defects in regulatory cells, as in the neonatal thymectomy models (44, 45).

In conclusion, these experiments show that the genetic background strongly conditions the manifestations of the defective self-tolerance resulting from a primary mutation in the *Aire* gene. In human populations, as in the inbred mice studied here, genetic polymorphism likely sets the range of organs for autoimmune attack and controls the severity of the disease that ensues. In this sense, the distinctions between monogenic and the typical polygenic autoimmune diseases become blurred.

MATERIALS AND METHODS

Mice. C57BL/6J, NOD/LtJ, BALB/cJ, SJL/J, NOD.H2^b, and B6.H2^{g7} mice were obtained from the Jackson Laboratory, and NOD.*Idd3*^{B6}.*Idd5*^{B10} mice (46) were obtained from Taconic Farms. All mice were housed and bred under specific pathogen-free conditions at the Harvard Medical School Center for Animal Resources and Comparative Medicine (Institutional Animal Care and Use Committee protocol 2954). The *Aire* knockout mutation, originally generated on a mixed (129/Sv × C57BL/6) F2 genetic background (20), was backcrossed onto the C57BL/6J (B6), NOD/LtJ (NOD), BALB/cJ (BALB/c), and SJL/J backgrounds for more than eight generations and intercrossed once for analysis. NOD.H2^b.*Aire*$^{-/-}$ and B6.H2^{g7}.*Aire*$^{-/-}$ strains were generated by crossing NOD.*Aire*$^{+/-}$ mice with NOD.H2^b (Jackson Laboratory) and B6.*Aire*$^{+/-}$ mice with B6.H2^{g7} mice, respectively. NOD.*Idd3/5*.*Aire*$^{-/-}$ strains were derived by backcrossing NOD.*Aire*$^{+/-}$ mice with NOD.*Idd3*^{B6}.*Idd5*^{B10} mice, selecting for *Idd3* and *Idd5* alleles before intercrossing. For the F1 and F2 analyses, NOD.*Aire*$^{+/-}$ males were bred with B6.*Aire*$^{+/-}$ females (both backcrossed for more than eight generations), and the resulting (B6 × NOD) F1.*Aire*$^{-/-}$ or *Aire*$^{+/-}$ mice were intercrossed to generate cohorts of (B6 × NOD) F2.*Aire*$^{-/-}$ mice. Mice were genotyped for the *Aire* mutation by PCR of tail DNA as described previously (20). The MHC haplotype was determined by allele-specific PCR for MHC-II A^b (5′-TCTAGAATTCACAGCGACATGGGCGAGC-3′ and 5′-TCTAGAATTCCGTAGTTGTGTCTGCACA-3′) or by staining peripheral blood lymphocytes with anti–I-A^b (AF6-120.1; BD Biosciences) and anti–I-A^{g7} (10–2.16). *Idd3*, *Idd5.1*, and *Idd5.2* alleles were typed by PCR using the following primer pairs: D3Mit21, D1Mit74, and D1Mit132 (available from the Mouse Genome Informatics Database).

Histopathology. Tissues were fixed in buffered 10% formalin and embedded with paraffin. Tissue sections were stained with hematoxylin and eosin and scored in a blinded fashion for lymphocytic infiltrates. In general, 0, 0.5, 1, 2, 3, and 4 indicate no, trace, mild, moderate, or severe lymphocytic infiltration, and complete destruction, respectively. For retinal degeneration, 1 = lesion present, but less than half of the photoreceptor layer lost; 2 = more than half of the photoreceptor layer lost; 3 = entire photoreceptor layer lost without or with mild outer nuclear layer attack; and 4 = the entire photoreceptor layer and most of the outer nuclear layer destroyed. For immunohistology, 5-μm frozen sections of eye, ovary, salivary, stomach, and pancreas were prepared from a 7-wk-old NOD.RAG-deficient mouse (to avoid Igs in the organs), incubated with 1:100 dilutions of sera, and counterstained with FITC-conjugated goat anti–mouse IgG (Jackson ImmunoResearch Laboratories).

Western blotting. Pancreas, salivary, and stomach tissue were homogenized on ice in a buffer containing 50 mM Tris, pH 8.0, 150 mM NaCl, 1% CHAPS, and a protease inhibitor cocktail (Roche Diagnostic). The homogenates were centrifuged at 13,000 revolutions per minute for 10 min, and the supernatants were mixed with a double volume of sample buffer (62.5 mM Tris-HCl, pH 6.8, 25% glycerol, 2% SDS, and 5% β-mercaptoethanol). The extracts were separated by 10% SDS-PAGE gel and electrophoretically transferred onto a polyvinylidene fluoride membrane (Bio-Rad Labortatories). The membranes were blocked with TBST (25 Mm Tris-HCl, pH 7.6, 150 mM NaCl, and 0.1% Tween 20) containing 5% nonfat milk for 1 h and assembled in a Mini-PROTEAN II Multiscreen apparatus (Bio-Rad Labortatories) and incubated overnight with 1:500 dilution of sera. After washing five times with TBST, the bound antibodies were reacted with horseradish peroxidase–conjugated donkey anti–mouse IgG (1:3,000; Jackson ImmunoResearch Laboratories) for 1 h and revealed with an enhanced chemiluminescence reagent (Pierce Chemical Co.) and autoradiography.

Genetic analysis. Genomic DNA was isolated from tail tips of 98 (B6 × NOD) F2*Aire*$^{-/-}$ mice by phenol-chloroform extraction and genotyped for SNP markers distinguishing B6 and NOD alleles, as previously described (5). Genetic analyses were performed with R/qtl and customized S-plus scripts for simple marker/trait association testing of dominant/additive/recessive effects (5). Experiment-wise p-values were established by permutation testing (1,000 permutations in R/qtl or S-Plus).

Online supplemental material. Table S1 shows histological score of (B6 × NOD) F2 Aire$^{-/-}$ mice. Table S2 shows the position and the trait/marker association score for each SNP tested in (B6 × NOD) F2 Aire$^{-/-}$ mice. Online supplemental material is available at http://www.jem.org/cgi/content/full/jem.20050693/DC1.

We would like to thank Whitney Besse for invaluable help with the genotyping; Vera Bruklich, Vanessa Tran, and Kimie Hattori for help with the mice; Alevtina Pinkhasov for help with the histology; and Vincent Butty and the Aire group for inspiring discussion.

This work was supported by a grant from the National Institutes of Health (NIH) and Young Chair funds to D. Mathis and C. Benoist, and by Joslin's National Institute of Diabetes and Digestive and Kidney Diseases–funded Diabetes Endocrine Research Center core facilities. W. Jiang received fellowship support from the American Diabetes Association, and M.S. Anderson received support from the Howard Hughes Medical Institute, the NIH, the Sandler Foundation, and the Pew Scholars Program.

The authors have no conflicting financial interests.

Submitted: 6 April 2005
Accepted: 10 August 2005

REFERENCES

1. Bach, J.F. 2002. The effect of infections on susceptibility to autoim-

mune and allergic diseases. *N. Engl. J. Med.* 347:911–920.
2. Kishimoto, H., and J. Sprent. 2001. A defect in central tolerance in NOD mice. *Nat. Immunol.* 2:1025–1031.
3. Liston, A., S. Lesage, D.H. Gray, L.A. O'Reilly, A. Strasser, A.M. Fahrer, R.L. Boyd, J. Wilson, A.G. Baxter, E.M. Gallo, et al. 2004. Generalized resistance to thymic deletion in the NOD mouse; a polygenic trait characterized by defective induction of Bim. *Immunity.* 21: 817–830.
4. Choisy-Rossi, C.M., T.M. Holl, M.A. Pierce, H.D. Chapman, and D.V. Serreze. 2004. Enhanced pathogenicity of diabetogenic T cells escaping a non-MHC gene-controlled near death experience. *J. Immunol.* 173:3791–3800.
5. Zucchelli, S., P. Holler, T. Yamagata, M. Roy, C. Benoist, and D. Mathis. 2005. Defective central tolerance induction in NOD mice: genomics and genetics. *Immunity.* 22:385–396.
6. Carrasco-Marin, E., J. Shimizu, O. Kanagawa, and E.R. Unanue. 1996. The class II MHC I-A^{g7} molecules from non-obese diabetic mice are poor peptide binders. *J. Immunol.* 156:450–458.
7. Ridgway, W.M., M. Fasso, and C.G. Fathman. 1999. A new look at MHC and autoimmune disease. *Science.* 284:749–751.
8. Stratmann, T., N. Martin-Orozco, V. Mallet-Designe, D. McGavern, G. Losyev, C. Dobbs, M.B.A. Oldstone, K. Yoshida, H. Kikutani, D. Mathis, et al. 2003. Susceptible MHC alleles, not background genes, select an autoimmune T cell reactivity. *J. Clin. Invest.* 112:902–914.
9. Kreuwel, H.T., J.A. Biggs, I.M. Pilip, E.G. Pamer, D. Lo, and L.A. Sherman. 2001. Defective CD8+ T cell peripheral tolerance in nonobese diabetic mice. *J. Immunol.* 167:1112–1117.
10. Luhder, F., J. Katz, C. Benoist, and D. Mathis. 1998. MHC class II molecules can protect from diabetes by positively selecting T cells with additional specificities. *J. Exp. Med.* 187:379–387.
11. Salomon, B., D.J. Lenschow, L. Rhee, N. Ashourian, B. Singh, A. Sharpe, and J.A. Bluestone. 2000. B7/CD28 costimulation is essential for the homeostasis of the $CD4^+CD25^+$ immunoregulatory T cells that control autoimmune diabetes. *Immunity.* 12:431–440.
12. Vijayakrishnan, L., J.M. Slavik, Z. Illes, R.J. Greenwald, D. Rainbow, B. Greve, L.B. Peterson, D.A. Hafler, G.J. Freeman, A.H. Sharpe, et al. 2004. An autoimmune disease-associated CTLA-4 splice variant lacking the B7 binding domain signals negatively in T cells. *Immunity.* 20:563–575.
13. Lyons, P.A., W.W. Hancock, P. Denny, C.J. Lord, N.J. Hill, N. Armitage, T. Siegmund, J.A. Todd, M.S. Phillips, J.F. Hess, et al. 2000. The NOD Idd9 genetic interval influences the pathogenicity of insulitis and contains molecular variants of Cd30, Tnfr2, and Cd137. *Immunity.* 13:107–115.
14. Wicker, L.S., M.C. Appel, F. Dotta, A. Pressey, B.J. Miller, N.H. Delarato, P.A. Fischer, R.C. Boltz Jr., and L.B. Peterson. 1992. Autoimmune syndromes in major histocompatibility complex (MHC) congenic strains of nonobese diabetic (NOD) mice: the NOD MHC is dominant for insulitis and cyclophosphamide-induced diabetes. *J. Exp. Med.* 176:67–77.
15. Braley-Mullen, H., G.C. Sharp, B. Medling, and H. Tang. 1999. Spontaneous autoimmune thyroiditis in NOD.H-2h4 mice. *J. Autoimmun.* 12:157–165.
16. Salomon, B., L. Rhee, H. Bour-Jordan, H. Hsin, A. Montag, B. Soliven, J. Arcella, A.M. Girvin, J. Padilla, S.D. Miller, and J.A. Bluestone. 2001. Development of spontaneous autoimmune peripheral polyneuropathy in B7-2–deficient NOD mice. *J. Exp. Med.* 194:677–684.
17. Koarada, S., Y. Wu, N. Fertig, D.A. Sass, M. Nalesnik, J.A. Todd, P.A. Lyons, J. Fenyk-Melody, D.B. Rainbow, L.S. Wicker, et al. 2004. Genetic control of autoimmunity: protection from diabetes, but spontaneous autoimmune biliary disease in a nonobese diabetic congenic strain. *J. Immunol.* 173:2315–2323.
18. Mathis, D., and C. Benoist. 2004. Back to central tolerance. *Immunity.* 20:509–516.
19. Ramsey, C., O. Winqvist, L. Puhakka, M. Halonen, A. Moro, O. Kampe, P. Eskelin, M. Pelto-Huikko, and L. Peltonen. 2002. Aire deficient mice develop multiple features of APECED phenotype and show altered immune response. *Hum. Mol. Genet.* 11:397–409.
20. Anderson, M.S., E.S. Venanzi, L. Klein, Z. Chen, S. Berzins, S.J. Turley, H. von Boehmer, R. Bronson, A. Dierich, C. Benoist, and D. Mathis. 2002. Projection of an immunological self shadow within the thymus by the aire protein. *Science.* 298:1395–1401.
21. Liston, A., S. Lesage, J. Wilson, L. Peltonen, and C.C. Goodnow. 2003. Aire regulates negative selection of organ-specific T cells. *Nat. Immunol.* 4:350–354.
22. Anderson, M.S., E.S. Venanzi, Z. Chen, S.P. Berzins, C. Benoist, and D. Mathis. 2005. The cellular mechanism of Aire control of T cell tolerance. *Immunity.* 23:227–239.
23. Ohashi, P.S. 2003. Negative selection and autoimmunity. *Curr. Opin. Immunol.* 15:668–676.
24. Venanzi, E.S., C. Benoist, and D. Mathis. 2004. Good riddance: thymocyte clonal deletion prevents autoimmunity. *Curr. Opin. Immunol.* 16:197–202.
25. Perheentupa, J. 1996. Autoimmune polyendocrinopathy–candidiasis–ectodermal dystrophy (APECED). *Horm. Metab. Res.* 28:353–356.
26. Betterle, C., N.A. Greggio, and M. Volpato. 1998. Autoimmune polyglandular syndrome type 1. *J. Clin. Endocrinol. Metab.* 83:1049–1055.
27. Halonen, M., P. Eskelin, A.G. Myhre, J. Perheentupa, E.S. Husebye, O. Kampe, F. Rorsman, L. Peltonen, I. Ulmanen, and J. Partanen. 2002. AIRE mutations and human leukocyte antigen genotypes as determinants of the autoimmune polyendocrinopathy-candidiasis-ectodermal dystrophy phenotype. *J. Clin. Endocrinol. Metab.* 87:2568–2574.
28. Concannon, P., K.J. Gogolin-Ewens, D.A. Hinds, B. Wapelhorst, V.A. Morrison, B. Stirling, M. Mitra, J. Farmer, S.R. Williams, N.J. Cox, et al. 1998. A second-generation screen of the human genome for susceptibility to insulin-dependent diabetes mellitus. *Nat. Genet.* 19: 292–296.
29. Lyons, P.A., N. Armitage, F. Argentina, P. Denny, N.J. Hill, C.J. Lord, M.B. Wilusz, L.B. Peterson, L.S. Wicker, and J.A. Todd. 2000. Congenic mapping of the type 1 diabetes locus, Idd3, to a 780-kb region of mouse chromosome 3: identification of a candidate segment of ancestral DNA by haplotype mapping. *Genome Res.* 10:446–453.
30. Hill, N.J., P.A. Lyons, N. Armitage, J.A. Todd, L.S. Wicker, and L.B. Peterson. 2000. NOD Idd5 locus controls insulitis and diabetes and overlaps the orthologous CTLA2/IDDM12 and NRAMP1 loci in humans. *Diabetes.* 49:1744–1747.
31. Broman, K.W., H. Wu, S. Sen, and G.A. Churchill. 2003. R/qtl: QTL mapping in experimental crosses. *Bioinformatics.* 19:889–890.
32. Kuroda, N., T. Mitani, N. Takeda, N. Ishimaru, R. Arakaki, Y. Hayashi, Y. Bando, K. Izumi, T. Takahashi, T. Nomura, et al. 2005. Development of autoimmunity against transcriptionally unrepressed target antigen in the thymus of Aire-deficient mice. *J. Immunol.* 174:1862–1870.
33. Boe, A.S., P.M. Knappskog, A.G. Myhre, J.I. Sorheim, and E.S. Husebye. 2002. Mutational analysis of the autoimmune regulator (AIRE) gene in sporadic autoimmune Addison's disease can reveal patients with unidentified autoimmune polyendocrine syndrome type I. *Eur. J. Endocrinol.* 146:519–522.
34. Buzi, F., R. Badolato, C. Mazza, S. Giliani, L.D. Notarangelo, G. Radetti, A. Plebani, and L.D. Notarangelo. 2003. Autoimmune polyendocrinopathy-candidiasis-ectodermal dystrophy syndrome: time to review diagnostic criteria? *J. Clin. Endocrinol. Metab.* 88:3146–3148.
35. Pearson, T., P. Weiser, T.G. Markees, D.V. Serreze, L.S. Wicker, L.B. Peterson, A.M. Cumisky, L.D. Shultz, J.P. Mordes, A.A. Rossini, and D.L. Greiner. 2004. Islet allograft survival induced by costimulation blockade in NOD mice is controlled by allelic variants of Idd3. *Diabetes.* 53:1972–1978.
36. Anderson, M.S., and J.A. Bluestone. 2005. The NOD mouse: a model of immune dysregulation. *Annu. Rev. Immunol.* 23:447–485.
37. Scire, G., F.M. Magliocca, S. Cianfarani, A. Scalamandre, V. Petrozza, and M. Bonamico. 1991. Autoimmune polyendocrine candidiasis syndrome with associated chronic diarrhea caused by intestinal infection and pancreas insufficiency. *J. Pediatr. Gastroenterol. Nutr.* 13:224–227.
38. Ward, L., J. Paquette, E. Seidman, C. Huot, F. Alvarez, P. Crock, E. Delvin, O. Kampe, and C. Deal. 1999. Severe autoimmune polyendocrinopathy-candidiasis-ectodermal dystrophy in an adolescent girl with a novel AIRE mutation: response to immunosuppressive therapy. *J.*

Clin. Endocrinol. Metab. 84:844–852.
39. Xu, B., N. Wagner, L.N. Pham, V. Magno, Z. Shan, E.C. Butcher, and S.A. Michie. 2003. Lymphocyte homing to bronchus-associated lymphoid tissue (BALT) is mediated by L-selectin/PNAd, α4β1 integrin/VCAM-1, and LFA-1 adhesion pathways. *J. Exp. Med.* 197:1255–1267.
40. Johnnidis, J.B., E.S. Venanzi, D.J. Taxman, J.P. Ting, C.O. Benoist, and D.J. Mathis. 2005. Chromosomal clustering of genes controlled by the aire transcription factor. *Proc. Natl. Acad. Sci. USA.* 102:7233–7238.
41. Kogawa, K., J. Kudoh, S. Nagafuchi, S. Ohga, H. Katsuta, H. Ishibashi, M. Harada, T. Hara, and N. Shimizu. 2002. Distinct clinical phenotype and immunoreactivity in Japanese siblings with autoimmune polyglandular syndrome type 1 (APS-1) associated with compound heterozygous novel AIRE gene mutations. *Clin. Immunol.* 103:277–283.
42. Turley, S., L. Poirot, M. Hattori, C. Benoist, and D. Mathis. 2003. Physiological β cell death triggers priming of self-reactive T cells by dendritic cells in a type-1 diabetes model. *J. Exp. Med.* 198:1527–1537.
43. Kojima, A., and R.T. Prehn. 1981. Genetic susceptibility to post-thymectomy autoimmune diseases in mice. *Immunogenetics.* 14:15–27.
44. Silveira, P.A., A.G. Baxter, W.E. Cain, and I.R. van Driel. 1999. A major linkage region on distal chromosome 4 confers susceptibility to mouse autoimmune gastritis. *J. Immunol.* 162:5106–5111.
45. Roper, R.J., R.D. McAllister, J.E. Biggins, S.D. Michael, S.H. Min, K.S. Tung, S.B. Call, J. Gao, and C. Teuscher. 2003. Aod1 controlling day 3 thymectomy-induced autoimmune ovarian dysgenesis in mice encompasses two linked quantitative trait loci with opposing allelic effects on disease susceptibility. *J. Immunol.* 170:5886–5891.
46. Robles, D.T., G.S. Eisenbarth, N.J. Dailey, L.B. Peterson, and L.S. Wicker. 2003. Insulin autoantibodies are associated with islet inflammation but not always related to diabetes progression in NOD congenic mice. *Diabetes.* 52:882–886.